

Status of a new evaluation of the neutron resonance parameters of ^{238}U at ORNL

Nuclear Data Group

Nuclear Science and Technology Division

Oak Ridge National Laboratory

H. DERRIEN, L.C. LEAL, and N.M. LARSON

OVERVIEW

- Introduction
- The experimental data base
- Method of analysis
- The resonance parameters
- The neutron cross sections
- Conclusion

Introduction

- Analysis performed in the framework of the U.S. DOE Nuclear Criticality Safety Program and of the Working Party on International Nuclear Data Evaluation Cooperation (WPEC).
- With the aim of solving current keff prediction problems and extending the resolved resonance range to 20 keV.
- SAMMY analysis of all the available ORELA experimental neutron transmission and neutron capture cross section data.

The experimental data base

Olsen et al. experimental neutron transmission data:

- 7 samples, 42 m flight path, energy range 5 eV to 10 keV, 1977;
- 4 samples, 150 m flight path, energy range 300 eV to 100 keV, 1979.

Harvey et al. experimental transmission data:

- 3 samples, 200 m flight path, energy range 1 keV to 1 MeV, 1988
- (the present work is the first analysis of the data); excellent resolution allowing the extension of the resolved resonance range to 20 keV.

De Saussure et al. effective capture cross section:

- sample thickness 0.0028 at/barn, 40 m flight path, 1973;
- resonances well resolved up to about 5 keV neutron energy;
- used in the higher energy range to check the calculated capture cross sections.

Macklin et al. effective capture cross section:

- 2 samples: 0.00309 at/b and 0.0124 at/b, 150 m flight path, 1988;
- Resolution similar to Harvey transmission;

Experimental capture cross section at 0.0253 eV:

- 2.68 b from Poenitz et al. 1981

Computer Code SAMMY

- Reich-Moore R-Matrix formalism;
- Baye's method of fit;
- Free gas model for Doppler broadening of the resonances;
- Gaussian experimental resolution plus exponential tail;
- Experimental effect corrections (background, normalization);
- Self-shielding and multiplescattering correction for the capture cross section (recently improved version of SAMMY).

Method

- Sequential analysis of up to 8 (depending on the energy range) experimental data sets, using the parameter covariance matrix from one sequence to the next;
- Preliminary fits of the transmission data for the determination of external resonance parameters leading to consistent values of the effective radius R' and of the normalization correction parameters, in agreement with the experimental normalization errors (less than 1%);
- Value obtained for R' : 9.45 ± 0.03 fm

The resonance parameters

Fits to the experimental data, in the energy range 0 to 20 keV, obtained by using:

- 932 s-wave resonances $J\pi = 1/2+$
- 814 p-wave resonances $J\pi = 1/2-$
- 1540 p-wave resonances $J\pi = 3/2-$

See on Fig.1 the plot of the number of resonances versus neutron energy. For both s and p resonances the average resonance spacing is nearly constant:

- $D0 = 21.5$ eV s-wave resonances
- $D1 = 8.5$ eV p-wave resonances

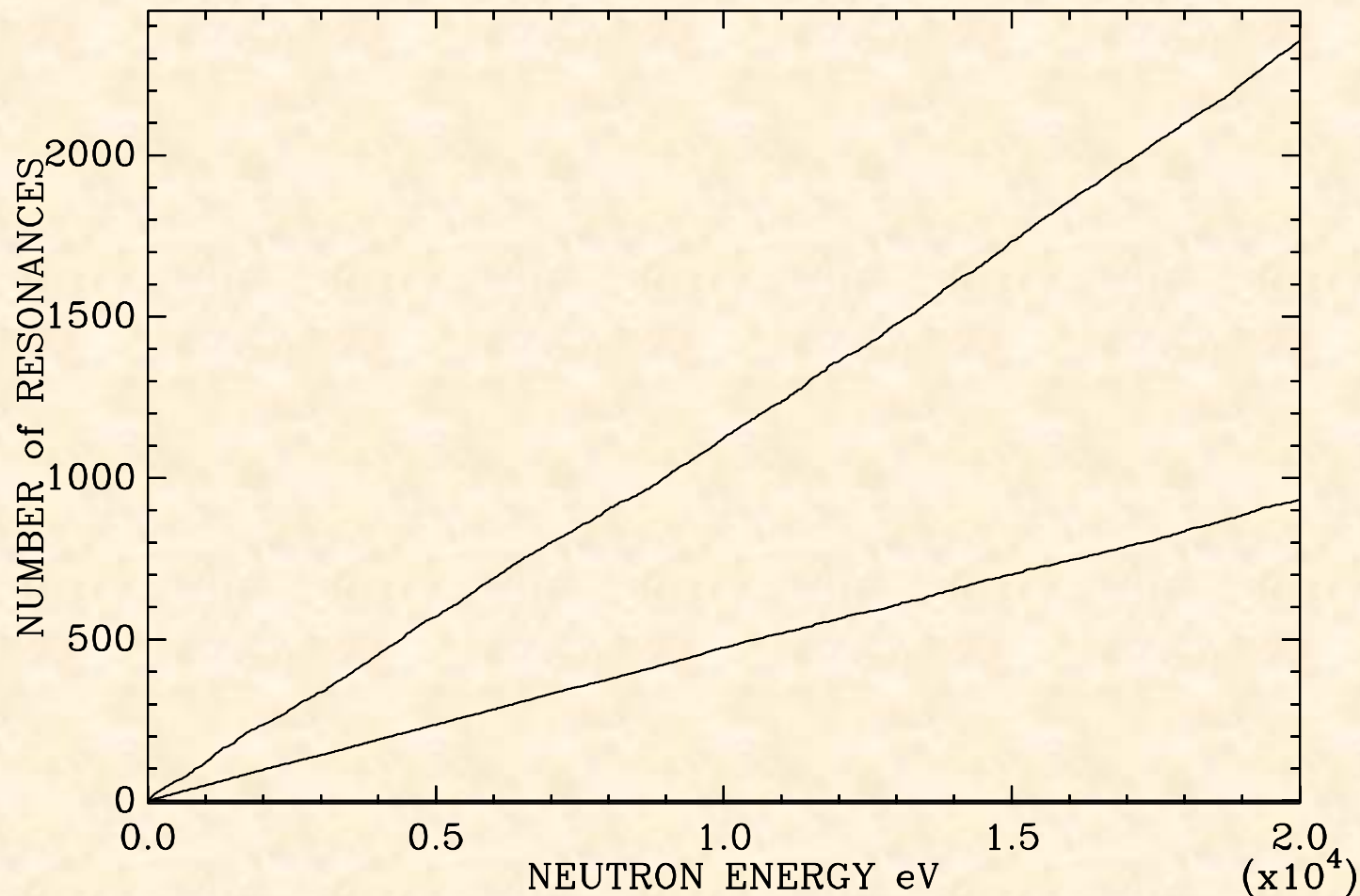
See on Fig. 2 and 3 the differential distribution of the level spacing:

- Fig. 2 s-wave resonances; one spin population; Wigner distribution;
- Fig. 3 p-wave resonances; two spin populations; superposition of two Wigner distributions

See on Fig.4 and 5 the differential distribution of the reduced neutron widths:

- Fig.4 s-wave reduced neutron widths, Porter-Thomas distribution
- Fig.5 p-wave reduced neutron widths, Porter-Thomas distribution
- Note the quite good agreement between the experimental and theoretical distributions

Figure 1. Number of resonances versus neutron energy. The upper line represents the p-wave resonances; the lower line represent the s-wave resonances.



The resonance parameters

Fits to the experimental data, in the energy range 0 to 20 keV, obtained by using:

- 932 s-wave resonances $J\pi = 1/2+$
- 814 p-wave resonances $J\pi = 1/2-$
- 1540 p-wave resonances $J\pi = 3/2-$

See on Fig.1 the plot of the number of resonances versus neutron energy. For both s and p resonances the average resonance spacing is nearly constant:

- $D_0 = 21.5$ eV s-wave resonances
- $D_1 = 8.5$ eV p-wave resonances

See on Fig. 2 and 3 the differential distribution of the level spacing:

- Fig. 2 s-wave resonances; one spin population; Wigner distribution;
- Fig. 3 p-wave resonances; two spin populations; superposition of two Wigner distributions

See on Fig.4 and 5 the differential distribution of the reduced neutron widths:

- Fig.4 s-wave reduced neutron widths, Porter-Thomas distribution
- Fig.5 p-wave reduced neutron widths, Porter-Thomas distribution
- Note the quite good agreement between the experimental and theoretical distributions

Figure 2. Differential distribution of the s-wave resonance spacing. The histogram represents the experimental data. The solid line represents the theoretical Wigner distribution.

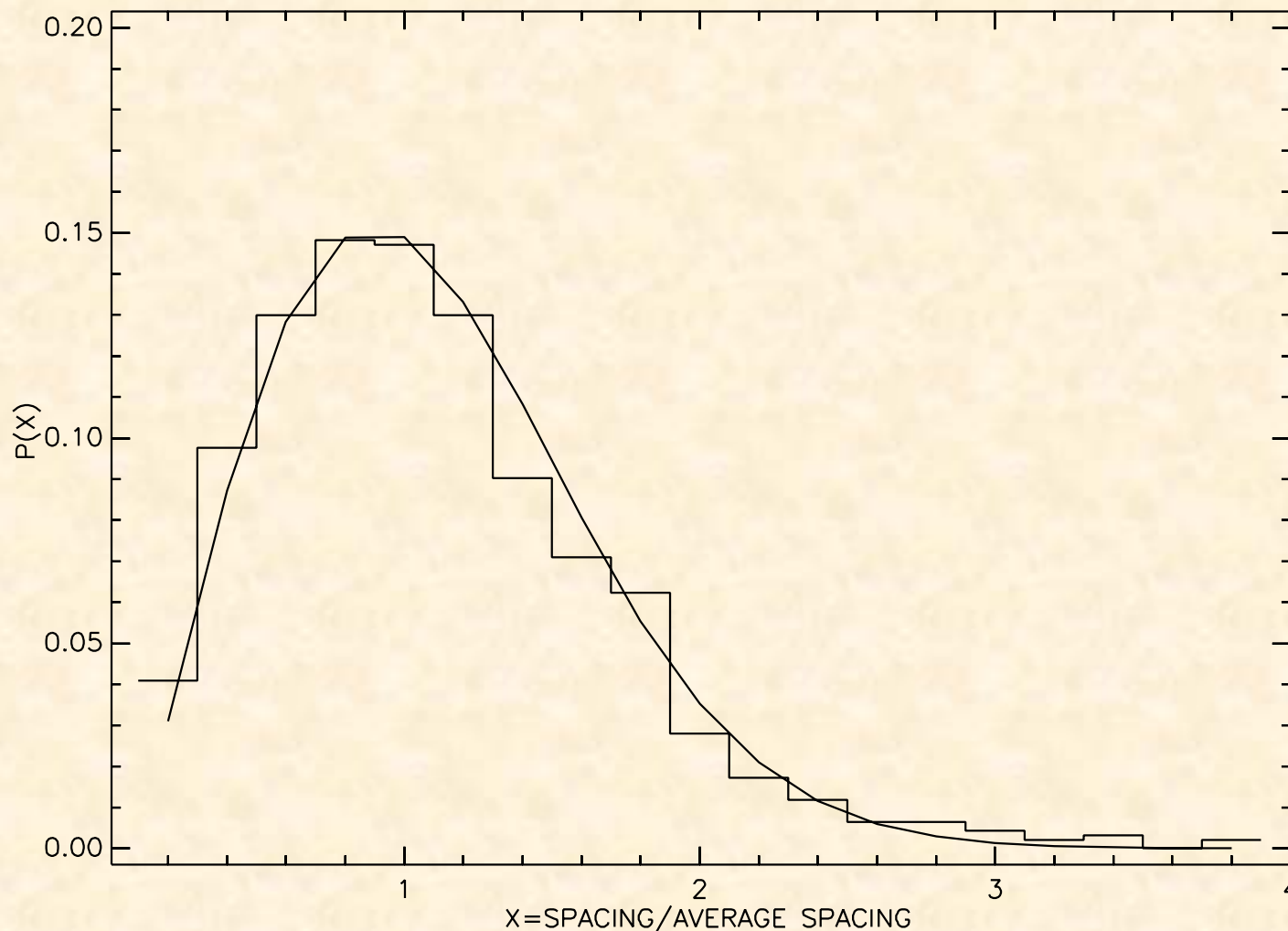
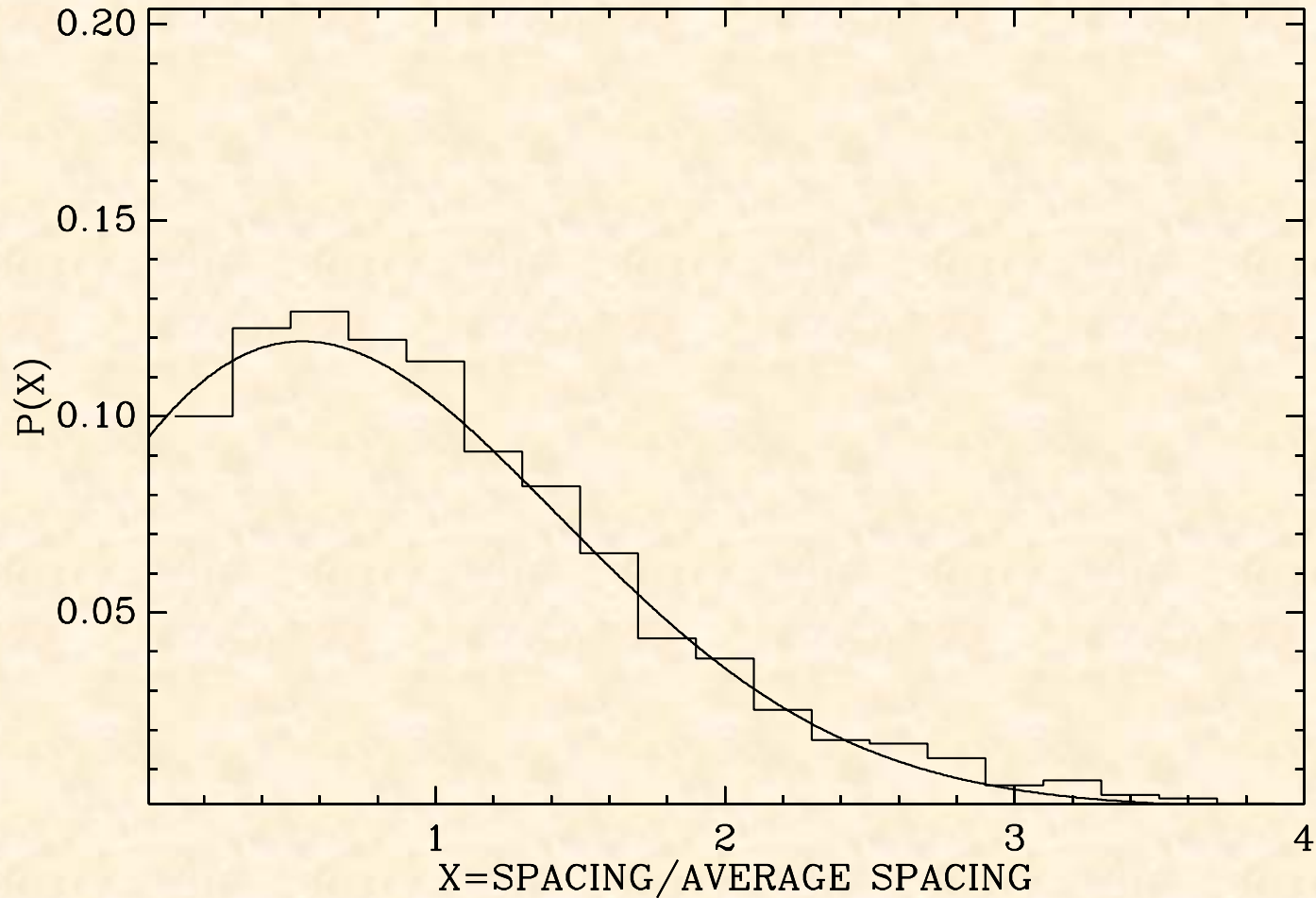


Figure 3. Differential distribution of the p-wave resonance spacings. The histogram shows the experimental distribution. The solid line represents the superposition of two Wigner distributions in the ratio of the population of the two p-wave spins.



The resonance parameters

Fits to the experimental data, in the energy range 0 to 20 keV, obtained by using:

- 932 s-wave resonances $J\pi = 1/2+$
- 814 p-wave resonances $J\pi = 1/2-$
- 1540 p-wave resonances $J\pi = 3/2-$

See on Fig.1 the plot of the number of resonances versus neutron energy. For both s and p resonances the average resonance spacing is nearly constant:

- $D_0 = 21.5$ eV s-wave resonances
- $D_1 = 8.5$ eV p-wave resonances

See on Fig. 2 and 3 the differential distribution of the level spacing:

- Fig. 2 s-wave resonances; one spin population; Wigner distribution;
- Fig. 3 p-wave resonances; two spin populations; superposition of two Wigner distributions

See on Fig.4 and 5 the differential distribution of the reduced neutron widths:

- Fig.4 s-wave reduced neutron widths, Porter-Thomas distribution
- Fig.5 p-wave reduced neutron widths, Porter-Thomas distribution
- Note the quite good agreement between the experimental and theoretical distributions

Figure 4. Differential distribution of the s-wave reduced neutron widths. The histogram represents the experimental distribution. The solid line is the Porter-Thomas distribution

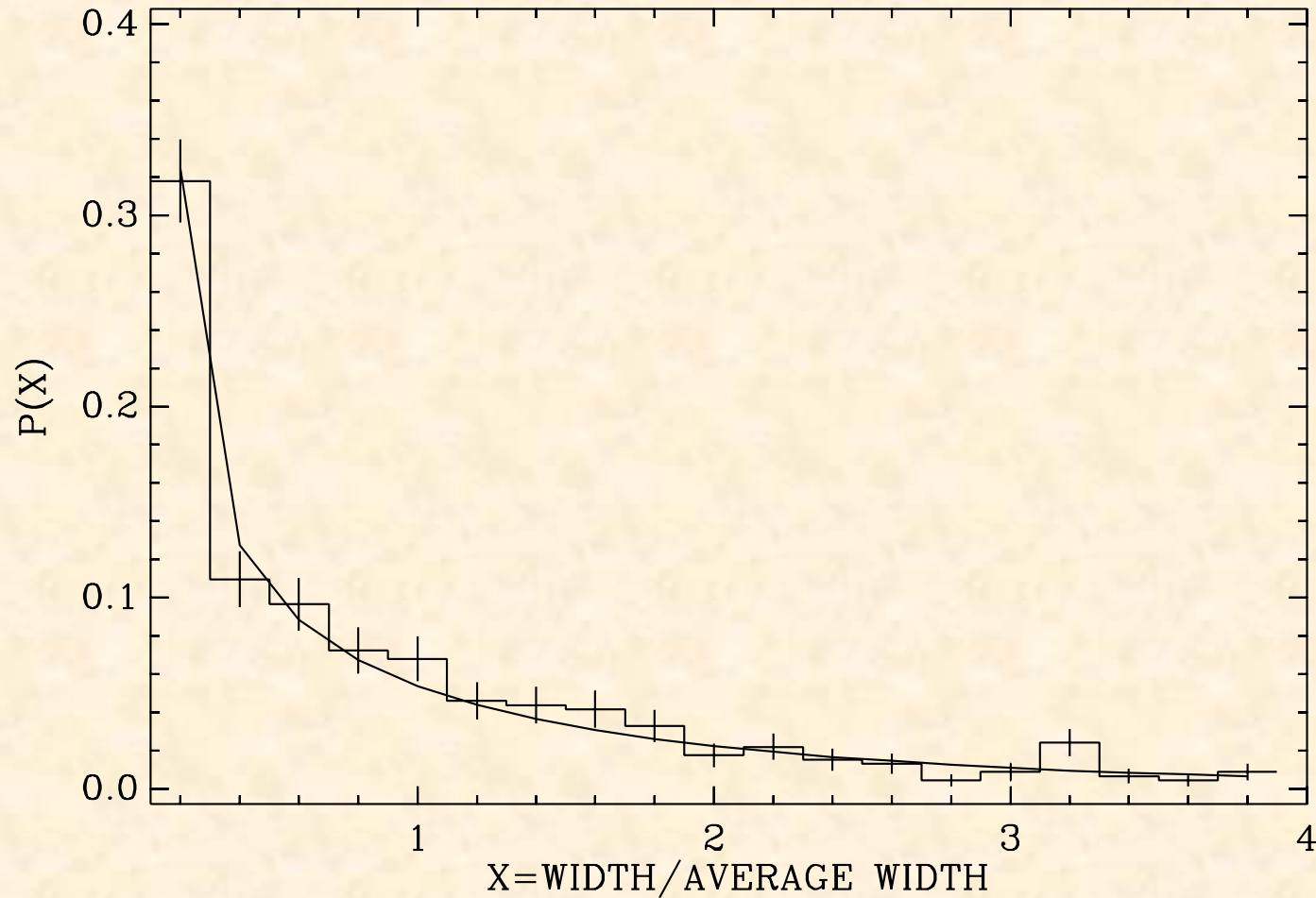
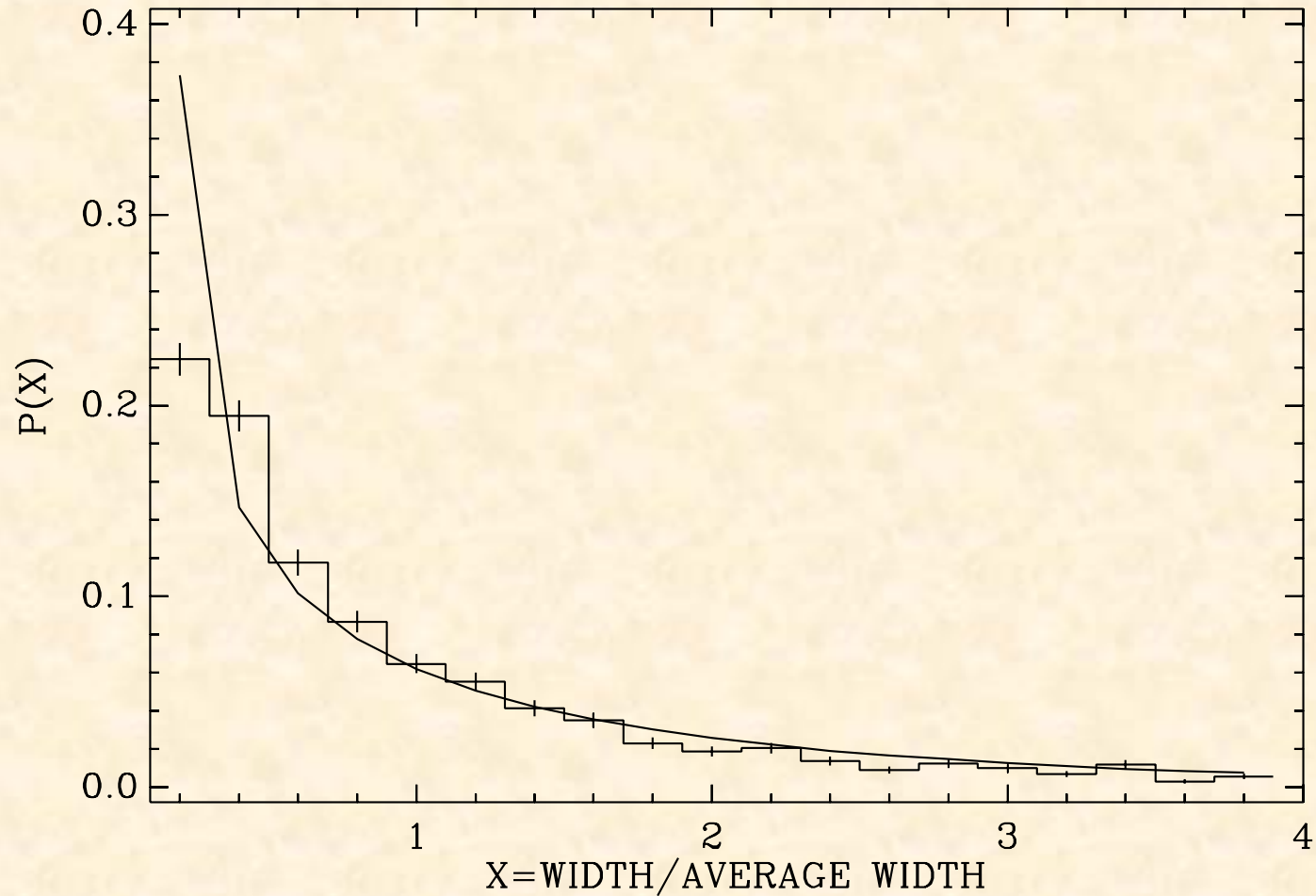


Figure 5. Differential distribution of the p-wave reduced neutron widths. The solid line is the Porter-Thomas distribution taking into account 15% of missing small neutron widths.



The calculated cross sections

Capture cross section at 0.0253 eV:

- 2.68 b, 1% smaller than ENDF/B-VI

Capture resonance integral:

- 275.0 b, 1% smaller than ENDF/B-VI

Capture cross section at higher energies:

- $\pm 2\%$ compared to ENDF/B-VI

Average elastic cross section:

- 2-3% higher than ENDF/B-V

Conclusion

- The ORNL ^{238}U resonance parameter file calculates smaller values of the thermal capture cross section and of the resonance capture integral, than the current evaluated files (ENDF/B-VI, JEF, JENDL...). The eigenvalues values for the LCT6 benchmarks are largely improved when using the ORNL parameters (calculations performed by MacFarlane (LANL) and Weinman (KAPL), for the WPEC working group).
- The ORNL ^{238}U resonance parameter file contain the resonance parameters of the energy range 10 keV to 20 keV obtained from the analysis of the Harvey high resolution transmission data, which will improve the accuracy of the self-shielding factors in this energy range.
- The evaluation is still in progress by adding to the experimental data base the high resolution experimental capture cross sections of Macklin et al. (ORELA, 1988) recently available. A good fit of Macklin data has been obtained.
- The resonance parameters in the energies 0 to 10 keV and 10 to 20 keV were merged in a single energy range 0 to 20 keV (parameters available for testing).

Example of a SAMMY fit of the effective total cross section of Harvey and capture cross section of Macklin

